J. Am. Chem. Soc. 1987, 109, 2341–2346

orthogonal orientation than the other three phenyl rings in the molecule. Such a change would reduce conjugation of this ring with the porphyrin aromatic π-system and distort the geometry of the molecule. The extent of such interactions remains speculation since there is no X-ray data or calculations as to the structure of 2-substituted 5,10,15,20-tetraphenylporphyrins.

Mechanism of Proton Transfer. The results of previous studies on tautomerism in symmetrical tetraarylporphyrins are consistent with simultaneous migration of the two protons involving a symmetrical transition state.[6] Large temperature-dependent deuterium isotope effects (48 ± 14 at 243 K) have been observed in a range of para-substituted tetraarylporphyrins.[6] The tautomerism is solvent, concentration, and aryl ring substituent independent[6] and above 200 K does not involve proton tunneling.[12]

Our data show that asymmetric porphyrins exhibit the same kinetic properties as the symmetrical porphyrins. Although our data show net two-proton transfer between the tautomers, the possibility of asynchronous movement on a molecular level cannot be excluded. An estimate of the kinetic isotope effect on k_1 (i.e., proton transfer from N-24 to N-21 and from N-22 to N-23) was obtained for 2-methoxy-5,10,15,20-tetraphenylporphyrin **9**. Line shape analysis of the N–H and methoxyl resonances of **9** was performed in the temperature range 200–235 K, while analysis of the methoxyl region of the deuteriated derivative produced values of k_1 in the range 245–285 K. An isotope effect of $k_H/k_D = 30 \pm 3$ at 242 K was obtained. This is comparable to the values reported for symmetrical tetraarylporphyrins[5c,6] and suggests that the transition-state structures for tautomerism in **1** and **2** are similar. Comparison of the activation parameters also strongly suggests that a similar mechanism operates in both systems.

Arrhenius plots of the kinetic data were linear over the range 200–300 K and show no evidence for proton tunneling. Hennig and Limbach[10] have proposed the existence of a temperature-independent (5.0 ± 0.5 s^{-1}) proton tunneling in 5,10,15,20-tetraphenylporphyrin **1**. Mosely and Stilbs[11] have argued against this proposal. The fact that in our work, exchange rates in 2-substituted porphyrins of less than 5 s^{-1} were measured (Tables I and II) by both DNMR and saturation transfer experiments implies that any temperature-independent tunneling is insignificant (on the NMR time scale) above 190 K. Proton tunneling in asymmetric systems involving an asymmetric double well potential is inherently less likely than in symmetrical systems, as only that part of the barrier which lies above both the initial and final states is available for tunneling.[27] This fact, taken together with the similarity of kinetic data in unsubstituted and 2-substituted tetraphenylporphyrins, further suggests that tunneling is absent in both systems.

Conclusions

(i) The tautomeric exchange, **2a** $\rightleftarrows$ **2b**, in 2-substituted 5,10,15,20-tetraphenylporphyrins involves two distinct exchange processes which are detectable by saturation transfer experiments and DNMR spectroscopy.

(ii) In all porphyrins studied, proton transfer involves a net two-proton transfer between tautomers in which the two hydrogens reside on diagonally opposite nitrogens.

(iii) Irrespective of the nature of the substituent, there is a directional preference for proton transfer N-24 $\rightleftarrows$ N-21 and N-22 $\rightleftarrows$ N-23; the alternative exchange N-24 $\rightleftarrows$ N-23 and N-21 $\rightleftarrows$ N-22 is much slower.

(iv) The cause of the observed directionality of the proton transfer has not been unequivocally established. The energy barriers show no obvious correlation to the electronic or steric nature of the substituent.

(v) The activation parameters for tautomerism in 2-substituted porphyrins **9–18** and an isotope effect in porphyrin **9** are essentially the same as those observed in symmetrical porphyrins. This suggests that the mechanism of proton transfer is similar in both symmetrical and asymmetrical systems.

(vi) No evidence for proton tunneling above 190 K was found.

(vii) The results obtained in this study show further that asymmetric porphyrins inherently provide more information on tautomerism than is available from the study of symmetrical porphyrins.

Acknowledgment. We thank the Australian Research Grants Scheme for financial support (to M.J.C.) and the Australian Government for a Commonwealth Postgraduate Award (to M. M.H.).

Registry No. 9, 95519-30-5; **10**, 82945-69-5; **11**, 82945-62-8; **12**, 102305-84-0; **13**, 81914-52-5; **14**, 42259-23-4; **15**, 82945-59-3; **16**, 102305-85-1; **17**, 102305-86-2; **18**, 102305-87-3.

Supplementary Material Available: Data used to obtain values in Tables II and III (17 pages). Ordering information is given on any current masthead page.

---

(27) Bell, R. P. *Chem. Soc. Rev.* **1974**, *3*, 513.

Kinetics of the Thermal Reduction of Methylviologen in Alkaline Aqueous and Methanolic Solutions

Vivian Novakovic and Morton Z. Hoffman*

Contribution from the Department of Chemistry, Boston University, Boston, Massachusetts 02215. *Received October 24, 1986*

Abstract: Methylviologen (MV^{2+}) is reduced to $MV^{\bullet+}$ in alkaline aqueous and methanolic solutions in the absence of air. In aqueous solution, the initial rate of $MV^{\bullet+}$ formation (R_i) obeys the following rate law: $R_i = k_{obsd}[MV^{2+}]^2[OH^-]^2$; $k_{obsd} = 0.12$ M^{-3} min^{-1} at 25.0 °C with $E_a = 58$ kJ mol^{-1}. A mechanism is proposed whereby the initial phase of the reaction occurs via the successive attack of OH^- on the 2- and 2′-positions of the aromatic rings, followed by the reduction of MV^{2+} by the electron-rich double pseudobase. In methanolic solution, the rate law is $R_i = k_{obsd}[MV^{2+}]^{1/2}[CH_3O^-]^2$; $k_{obsd} = 4.9 \times 10^2$ M$^{-3/2}$ min^{-1} at 25.0 °C with $E_a = 95$ kJ mol^{-1}. It is suggested that MV^{2+} exists in methanolic solutions at the concentrations employed mainly as a dimeric aggregate, $(MV^{2+})_2$. the proposed mechanism involves an equilibrium between MV^{2+} and $(MV^{2+})_2$, with only MV^{2+} being reactive toward the formation of the pseudobase with CH_3O^-. Exposure of $MV^{\bullet+}$ to O_2 results in the formation of luminescent (λ_{em} 525 nm) and absorbing (λ_{max} ~380 nm) species via secondary reactions involving H_2O_2, which is formed slowly from the disproportionation of $O_2^{\bullet-}$.

Methylviologen (1,1′-dimethyl-4,4′-bipyridinium dication; MV^{2+}) is the archetypical electron relay in systems that serve as models for the photochemical storage and conversion of solar energy;[1] in addition, MV^{2+} is an important herbicide[2] and bio-

0002-7863/87/1509-2341$01.50/0

Scheme I

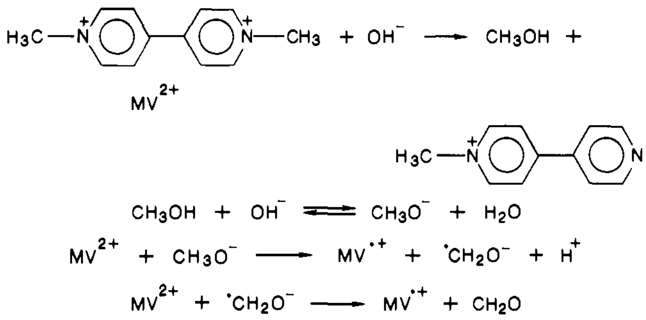

logical oxidation–reduction indicator.[3] The one-electron reduction of MV^{2+} to $MV^{\bullet+}$ is reversible and occurs with $E^0 = -0.44$ V vs. NHE in water.[4]

It has been known for a long time that MV^{2+} is thermally reduced to $MV^{\bullet+}$ (λ_{max} 395, 605; ϵ_{395} and $\epsilon_{605} = 4.21 \times 10^4$ and 1.37×10^4 M^{-1} cm^{-1})[5] in the absence of air in highly alkaline aqueous and alcoholic solutions.[6] Farrington et al.[7] proposed that the reaction occurs via Scheme I in which OH^- induces the dequaternization of MV^{2+} to generate CH_3OH; in deaerated alkaline solution, the resulting CH_3O^- is regarded as capable of reducing MV^{2+} to $MV^{\bullet+}$, yielding the reducing $^\bullet CH_2O^-$ radical that leads to a second equivalent of $MV^{\bullet+}$. The mechanism was supported by the observation of the acceleration of the formation of $MV^{\bullet+}$ in deaerated neat or aqueous methanolic solutions and the formation of 1-methyl-4-(4-pyridyl)pyridinium cation as a product upon the acidification of the solution and exposure to air.

When air is present initially, alkaline solutions of MV^{2+} slowly turn pale yellow, and $MV^{\bullet+}$ does not accumulate until the O_2 in the solution is depleted. Scheme II, proposed to account for the production of luminescent and UV-absorbing mono- and bipyridones when the reaction takes place in the presence of air,[8] involves the initial attack of OH^- at the 2-position of one of the aromatic rings to yield a pseudobase which, upon deprotonation of the newly formed alcohol, reduces successively 2 equiv of MV^{2+}. The formation of pseudobases or covalent hydrates from the interaction of nucleophiles with N-aromatic heterocycles is well established.[9] However, in the case of the interaction of OH^- with MV^{2+}, the direct observation of a pseudobase or other intermediates has not been successful.[10]

Apparently, the only quantitative examination to date of the kinetics of the thermal reduction was performed by Baker and Casadevall[11] in a study designed as an undergraduate laboratory exercise. They measured the time from the mixing of the reagents to the appearance of $MV^{\bullet+}$ as a function of $[MV^{2+}]$, $[OH^-]$, and $[CH_3CH_2OH]$ in air-saturated aqueous ethanolic solution; a first-, second-, and greater than fifth-order dependence was found for the respective species. Inasmuch as the appearance of $MV^{\bullet+}$ occurs only when all the O_2 in the solution has been scavenged, it is not possible to relate these results to the situation in the absence of air. In fact, these authors were unable to suggest a mechanism beyond those proposed earlier.[7,8]

Scheme II

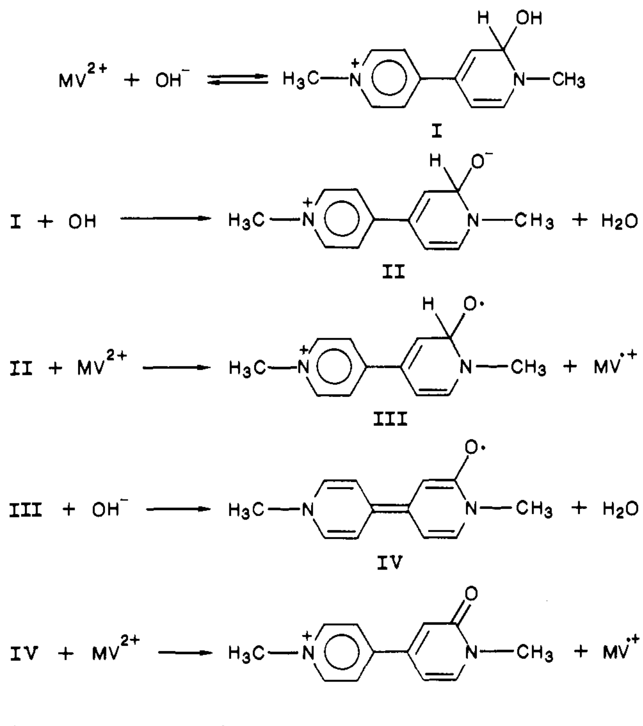

Recently, the rate of exchange of the 2,2′,6,6′-hydrogens of MV^{2+} with D_2O in alkaline solution was measured by the use of NMR;[12] the observed rate law of the reaction was first-order, with k_{obsd} proportional to $[OD^-]$. The authors stated that the exchange and reduction reactions appear to occur via independent mechanisms; in that case there would be no relation between the exchange kinetics and those of the reduction reaction.

Because the mechanism of the thermal reduction of MV^{2+} in highly alkaline solution has not been securely established, and because MV^{2+} has been used in a number of photochemical applications in that medium,[13-15] we have investigated the kinetics of the reaction in alkaline aqueous, methanolic, and mixed aqueous–methanolic solutions in the absence of O_2; the behavior of the systems upon exposure to O_2 has also been examined. In this paper we report on our determination of the rate of the initial formation of $MV^{\bullet+}$ as a function of the various solution medium parameters and temperature; we have established the rate laws for the reactions, evaluated the rate constants, and determined the activation parameters. From these results, mechanisms for the reactions are proposed. In addition, information is presented regarding the luminescence from MV^{2+} solutions,[16,17] the genuineness of which has been previously questioned.[18,19]

Experimental Section

Materials. Methylviologen dichloride (B.D.H.) was recrystallized 3 times from methanol and dried at 70 °C under vacuum for 24 h. NaOH and Na_2SO_4 (analytical grade) were used without additional purification. Aqueous and methanolic solutions of methylviologen were prepared using distilled water, which had been passed through a Millipore purification train, and anhydrous methanol (acetone-free; 99.94% by volume; Mallinckrodt), respectively. All methylviologen solutions were prepared immediately before use. A ~2 M NaOH stock solution, standardized against potassium acid phthalate primary standard, was used for the preparation of all aqueous NaOH solutions. Methanolic NaOH solutions were made from a ~6 mM stock solution.

---

(1) *Photogeneration of Hydrogen*; Harriman, A., West, M. A., Eds.; Academic: London, 1982 and references therein.

(2) Summers, L. A. *The Bipyridinium Herbicides*; Academic: London, 1980.

(3) Naik, M. S.; Nicholas, D. J. D. *Biochim. Biophys. Acta* **1967**, *131*, 204.

(4) Michaelis, L. *Biochem. Z.* **1932**, *250*, 564.

(5) Watanabe, T.; Honda, K. *J. Phys. Chem.* **1982**, *86*, 2617.

(6) Ledwith, A. *Acc. Chem. Res.* **1972**, *5*, 133 and references therein.

(7) Calderbank, A.; Charlton, D. F.; Farrington, J. A.; James, R. *J. Chem. Soc., Perkin Trans. 1* **1972**, 138.

(8) Farrington, J. A.; Ledwith, A.; Stam, M. F. *J. Chem. Soc., Chem. Commun.* **1969**, 259.

(9) Albert, A. *Adv. Heterocycl. Chem.* **1976**, *20*, 117.

(10) Rieger, A. L.; Rieger, P. H. *J. Phys. Chem.* **1984**, *88*, 5845.

(11) Baker, A. D.; Casadevall, A. *J. Chem. Educ.* **1980**, *57*, 515.

(12) Rieger, A. L.; Edwards, J. O. *J. Org. Chem.* **1985**, *50*, 5102.

(13) Okura, I.; Kim-Thuan. N.; Takeuchi, M. *Inorg. Chim. Acta* **1981**, *53*, L149.

(14) Okura, I.; Kim-Thuan, N.; Takeuchi, M. *Inorg. Chim. Acta* **1982**, *57*, 257.

(15) Xu, J.-G.; Porter, G. B. *Can. J. Chem.* **1982**, *60*, 2856.

(16) Polous, A. T.; Kelley, C. K. *J. Chem. Soc., Faraday Trans. 1* **1983**, *79*, 55.

(17) Kuczynski, J. P.; Milosavljevic, B. H.; Lappin, A. G.; Thomas, J. K. *Chem. Phys. Lett.* **1984**, *104*, 149.

(18) Hoffman, M. Z.; Prasad, D. R.; Jones, G., II; Malba, V. *J. Am. Chem. Soc.* **1983**, *105*, 6360.

(19) Prasad, D. R.; Hoffman, M. Z. *J. Phys. Chem.* **1984**, *88*, 5660.

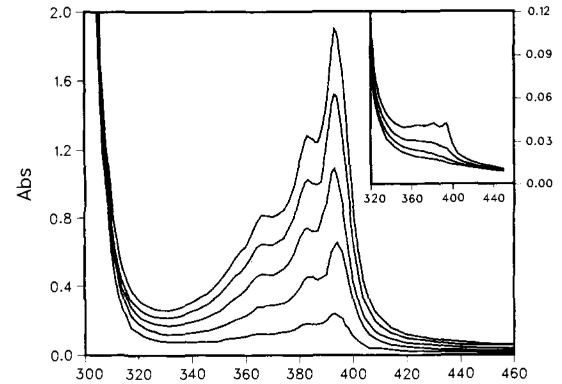

Figure 1. Spectra (1-cm cell) as a function of time (20.5, 28.5, 36.5, 44.5, and 52.0 min after mixing) of a deaerated solution containing initially 7.5 mM MV^{2+} and 0.50 M NaOH. Inset: 3.0, 6.5, 10.0, and 13.5 min after mixing.

Apparatus. UV–vis absorption spectra were recorded on Cary 118 and 210 spectrophotometers. A thermostat was used to maintain the temperature of the cell compartment at 25.0 ± 0.1 °C, unless otherwise specified. The sample solutions were contained in 1-cm quartz cuvettes that possessed a greaseless vacuum stopcock. Emission and excitation spectra were recorded on a Perkin-Elmer MPF-2A spectrofluorimeter at ambient temperature. For illumination of the solutions, the full intensity of a 1000-W quartz-jacketed xenon arc lamp was used.

Procedures. For deaerated solutions, a glass syringe was used to inject 2.0 mL of a neutral aqueous or methanolic MV^{2+} solution of known concentration into the cuvette. A continuous flow of Ar gas was bubbled through the solution for 10 min after which time the solution was deaerated and the stopcock was closed. In order to ensure that air would not leak into the system, the ends of the stopcock and the neck of the cuvette were sealed with plastic film. Approximately 5 mL of an aqueous or methanolic NaOH solution of known concentration was contained in a flask which was sealed with a rubber septum through which passed two stainless steel needles. Ar was bubbled through one of the needles and into the solution for 10 min. Two milliliters of the NaOH solution were withdrawn from the flask with the glass syringe and were injected into the cuvette containing the MV^{2+} solution through the stopcock. The time of mixing was taken as the zero time of the reaction. Ar was bubbled through the reaction mixture for ~2 min to ensure that the sample solution was homogeneous and that any residual oxygen had been removed; the blue color formed uniformly throughout the entire reaction mixture. The stopcock was closed, and the neck of the flask was resealed with plastic film. The rate of the reaction was followed by the monitoring of the absorption of the solution at 39 and/or 605 nm as a function of time.

For solutions saturated with O_2, equal volumes of aqueous MV^{2+} and NaOH were mixed together in a 1-cm quartz cuvette. A steady stream of O_2 was bubbled through the solution between successive absorption measurements to ensure that saturation was achieved.

Results

Aqueous Solutions. When an initially neutral solution of MV^{2+} (7.5 mM) is made highly alkaline ([NaOH] = 0.50 M), the tail absorption of MV^{2+} in the 320–400-nm region is immediately enhanced slightly, an effect very similar to that observed when Cl^- is added to MV^{2+}. During the next several minutes, under deaerated conditions, the tail absorption increases and shows a broad feature at ~380 nm from which subsequently emerges the structured spectrum characteristic of $MV^{\bullet+}$ (Figure 1). After the initial induction period, which is attributed to the scavenging of residual O_2 by $MV^{\bullet+}$, the $MV^{\bullet+}$ absorption increases linearly with time (Figure 2); from a knowledge of the slope of the line and ϵ at the monitoring wavelength (395 nm), a value of the initial rate of formation of $MV^{\bullet+}$ (R_i) can be calculated. The value of R_i is identical if the absorbance change at 605 nm is monitored. The induction period can be shortened or eliminated by the illumination of the reaction mixture; R_i is not affected by this action. The length of the induction period is also decreased when R_i is increased.

R_i changes when the initial concentrations of either MV^{2+} or NaOH, or the temperature, are varied; Table I shows the average values of R_i as a function of these parameters. In those experiments where $[OH^-]$ was varied at constant $[MV^{2+}]$, adjustment of the ionic strength of the solution to 1.0 M with Na_2SO_4 or NaCl yielded the same rate.

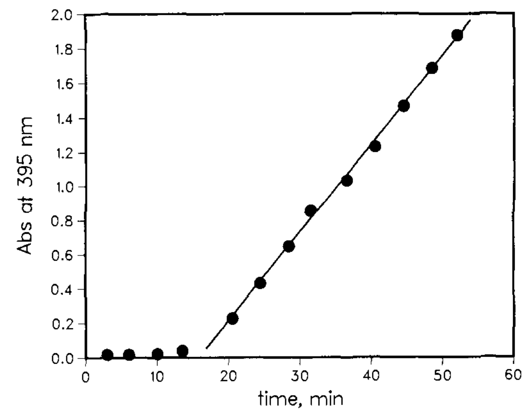

Figure 2. Absorbance at 395 nm (1-cm cell) as a function of time of a deaerated solution containing initially 7.5 mM MV^{2+} and 0.50 M NaOH.

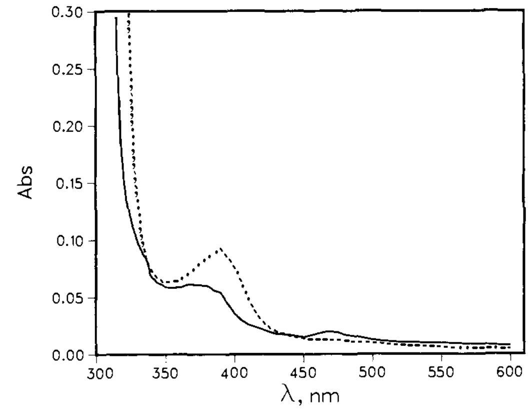

Figure 3. Spectra (1-cm cell) of solutions containing initially 7.5 mM MV^{2+} and 0.50 M NaOH. Deaerated for 30 min and then bubbled with O_2 (—); bubbled continuously for 30 min (---).

Table I. Values of R_i as a Function of $[MV^{2+}]$ and [NaOH] in Aqueous Solution

T, °C	$[MV^{2+}]$, mM	[NaOH], M	R_i,[a] μM min^{-1}
15.0	7.5	0.50	0.55
25.0	1.0	0.50	0.046
	5.0	0.50	0.70
	7.5	0.50	1.6, 1.2[b]
	10	0.50	2.4
	7.5	0.050	0.10[c]
	7.5	0.075	0.16, 0.042[b]
	7.5	0.10	0.18, 0.092[b]
	7.5	0.25	0.56, 0.32[b]
	7.5	1.0	6.9
40.0	7.5	0.50	4.9
55.0	7.5	0.50	13
70.0	7.5	0.50	27

[a] Average value from 2–18 individual runs; average deviation ± 10%. [b] Ionic strength adjusted to 1.0 M with Na_2SO_4. [c] Average deviation ± 30%.

When O_2 is bubbled through an initially deaerated solution containing 7.5 mV MV^{2+} and 0.50 M NaOH after 30 min (corresponding to the generation of ~20 μM $MV^{\bullet+}$), the absorption spectrum of $MV^{\bullet+}$ is replaced by that shown in Figure 3; for comparison, the absorption spectrum obtained for an identical solution continuously bubbled with O_2 for the same length of time is also shown. Both solutions exhibit similar emission and excitation spectra (Figure 4); it should be noted that freshly prepared neutral solutions of MV^{2+} exhibit weak excitation and emission bands at 400 and 525 nm, respectively. When alkaline solutions are continuously bubbled with O_2, the emission and excitation bands grow simultaneously and linearly with time. A

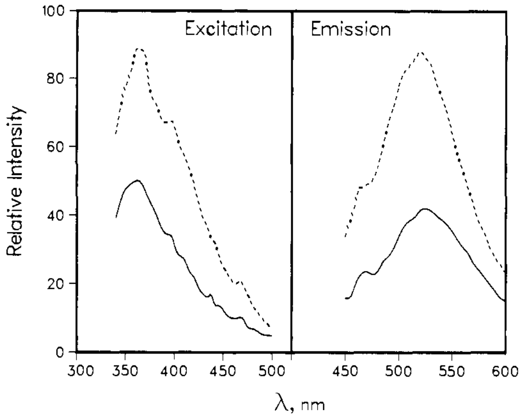

Figure 4. Emission (λ_{ex} 400 nm) and excitation (λ_{em} 520 nm) spectra of solutions containing initially 7.5 mM MV^{2+} and 0.50 M NaOH. Deaerated for 30 min and then bubbled with O_2 (—); bubbled continuously for 30 min (- - -).

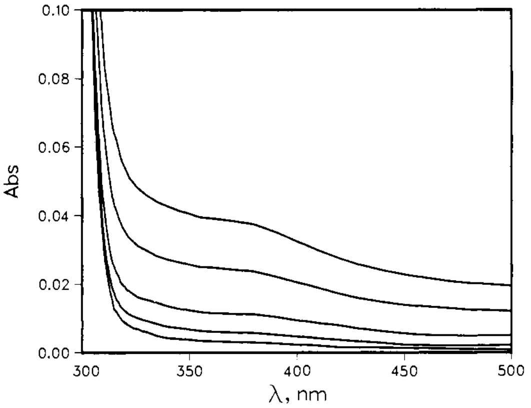

Figure 5. Spectra (1-cm cell) as a function of time (15, 30, 60, 105, and 165 min after mixing) of a O_2-saturated solution containing initially 0.50 mM MV^{2+} and 0.50 M NaOH.

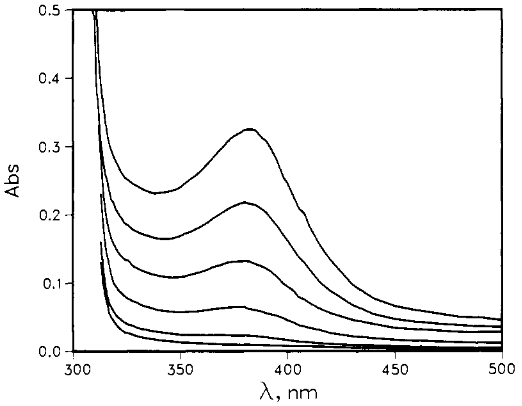

Figure 6. Spectra (1-cm cell) as a function of time (1, 16, 36, 56, 77, and 97 min after mixing) of a O_2-saturated solution containing initially 5.0 mM MV^{2+} and 0.50 M NaOH.

linear increase in the tail absorption is first observed as a function of time (Figure 5), followed by the accelerating growth of a discrete absorption band at 380 nm (Figure 6). At constant $[OH^-]$ (0.50 M), the rate of the initial growth of the tail absorption is approximately proportional to $[MV^{2+}]$ (0.20–5.0 mM); at constant $[MV^{2+}]$ (2.0 mM), this rate is virtually independent of $[OH^-]$ (0.050–0.50 M).

Methanolic Solutions. The rate of the thermal reduction of MV^{2+} is significantly greater in alkaline methanol compared with water at the same substrate concentrations. As a result, lower concentrations of MV^{2+} and NaOH had to be employed. The growth of the absorption spectrum of $MV^{\bullet+}$ was linear with time after the initial induction period; the general behavior of the system was the same as observed in aqueous solution. Table II presents the average values of R_i as a function of $[MV^{2+}]$, [NaOH], and temperature.

Table II. Values of R_i as a function of $[MV^{2+}]$ and [NaOH] in Methanolic Solution

T, °C	$[MV^{2+}]$, mM	[NaOH], mM	R_i,[a] μM min^{-1}
15.0	0.10	0.50	0.21
25.0	0.10	0.20	0.12
	0.10	0.50	1.2[b]
	1.0	0.50	5.1
	5.0	0.50	6.6
	10	0.50	11
	0.10	0.80	3.6
	0.10	2.0	11
35.0	0.10	0.50	3.1
45.0	0.10	0.50	9.6

[a] Average value from 2–9 individual runs; average deviation ± 10%. [b] Average deviation ± 30%.

Table III. Values of R_i as a Function of X_m in Aqueous Methanolic Solutions

X_m	$[MV^{2+}]$, mM	[NaOH], mM	R_i,[a] μM min^{-1}
0.00	7.5	50	0.10[b]
0.10	7.5	50	0.082[c]
0.16	7.5	50	0.26
0.23	7.5	50	2.5
0.40	7.5	50	28
0.51	10	0.50	0.046
0.64	10	0.50	0.20
0.80	10	0.50	1.5
1.00	10	0.50	11

[a] Average value from 2–4 individual runs; average deviation ± 10%. [b] Average deviation ± 30%. [c] Average deviation ± 15%.

Solutions initially deaerated and then purged with O_2 after 30 min or continuously bubbled with O_2 showed the appearance of weak absorption bands at ~390 and ~460 nm; emission at 525 nm with excitation bands at 400–450 nm was also detected.

Table III shows that R_i generally increases as the mole fraction of methanol (X_m) in aqueous solutions is increased at constant $[MV^{2+}]$ and [NaOH]; the sharp increase in R_i at $X_m = 0.4$ necessitated a lowering of the concentrations. Interestingly, small fractions of methanol in water do not have a significant effect, while the presence of a small amount of water in methanol produces a marked decrease in the value of R_i.

Discussion

Qualitatively, our observations on the reduction of MV^{2+} in alkaline solution are the same as those reported previously by others: the acceleration of the rate in the presence of methanol, the generation of absorbing and emitting products in the presence of air, and the general dependence of the rate on the concentrations of the reacting species. In addition, it is quite clear that OH^- forms ion-pair complexes with MV^{2+} in aqueous solution; it is to be anticipated that CH_3O^- does the same in methanol, perhaps to a greater extent due to the lower dielectric constant of that solvent. Because of the competing thermal reaction and the accompanying spectral changes, it was not possible to determine the equilibrium constants of formation of the ion-pair complexes; as a first approximation, we can assume that K_{eq} for the formation of $[MV^{2+}\cdots OH^-]$ is of the order of 1–3 M^{-1} in aqueous solution by analogy with complexes of other uninegative anions (Cl^-, Br^-, I^-, SCN^-) with MV^{2+}.[20,21]

Inasmuch as the extent of conversion of MV^{2+} to $MV^{\bullet+}$ is always <1%, the order of the reaction can be evaluated by van't Hoff's method[22] in which the initial rate of the reaction is determined as a function of the initial concentration of one of the

---

(20) Ebbesen, T. W.; Ferraudi, G. *J. Phys. Chem.* **1983**, *87*, 3717.

(21) Ebbesen, T. W.; Manring, L. E.; Peters, K. S. *J. Am. Chem. Soc.* **1984**, *106*, 7400.

(22) Moore, J. W.; Pearson, R. G. *Kinetics and Mechanism*, 3rd ed.; Wiley: New York, 1981; p 65.

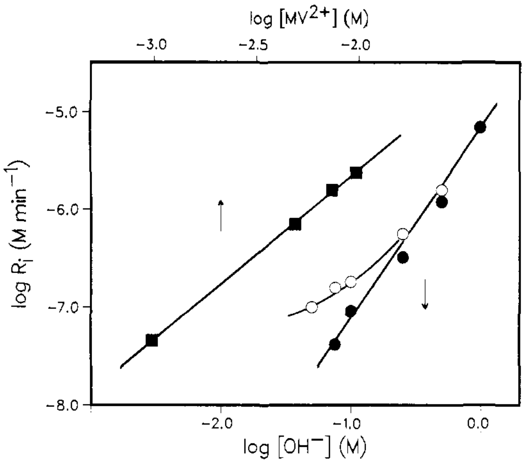

Figure 7. Plot of log R_i (at 25.0 °C) vs. log [MV^{2+}] at constant [OH^-] (0.50 M) (■) or vs. log [OH^-] at constant [MV^{2+}] (7.5 mM) (●, 1.0 M ionic strength; ○, ambient ionic strength). Data taken from Table I.

components when the initial concentrations of the other components are kept constant. The slope of the plot of log R_i vs. log (concentration of the varying component) gives the order of the reaction with respect to that component.

Figure 7 shows these plots for the data in Table I for aqueous solutions at 25.0 °C; the data at constant ionic strength indicate that the reaction is second-order in both MV^{2+} and OH^-: $R_i = k_{obsd}[MV^{2+}]^2[OH^-]^2$. From the measured values of R_i and the initial concentrations of the components, an average value of k_{obsd} of 0.12 M^{-3} min^{-1} (average deviation = 0.02) is obtained for the 24 individual runs at 25.0 °C in which the ionic strength is ambient with 0.50 M NaOH or adjusted to 1.0 M. Figure 7 demonstrates that R_i is not very sensitive to small differences at high ionic strengths. The values of K_{obsd} at 15.0, 40.0, 55.0, and 70.0 °C from the data in Table I are 0.038, 0.34, 0.88, and 1.9 M^{-3} min^{-1}, respectively; a plot of ln k_{obsd} vs. $1/T$ is linear and yields E_a = 58 kJ mol^{-1}.

A similar treatment of the data in Table II for methanolic solutions, albeit not at constant ionic strength, at 25.0 °C demonstrates that the reaction is one-half-order in MV^{2+} and second-order in OH^-; inasmuch as CH_3O^- is the basic species in alkaline methanol, the rate law can be written as $R_i = k_{obsd}[MV^{2+}]^{1/2}[CH_3O^-]^2$. The values of k_{obsd} at 15.0, 25.0, 35.0, and 45.0 are 8.2×10^1, 4.9×10^2, 1.2×10^3, and 3.8×10^3 $M^{-3/2}$ min^{-1}, repectively, corresponding to E_a = 95 kJ mol^{-1}.

Concerning the reaction in aqueous solutions, an analysis of the mechanism in Scheme I upon application of the steady-state approximation for $\cdot CH_2O^-$, CH_3O^-, and CH_3OH yields a rate law that is first-order in both MV^{2+} and OH^-; the same form of the rate law is obtained if the second reaction is treated as going to completion. The mechanism in Scheme II yields a rate law that is first-order in MV^{2+} and second-order in OH^- when the steady-state approximation is applied to intermediates I–IV; if the mechanism is modified with the initial reaction going to completion, the rate law becomes first-order in both reactants. Inasmuch as neither scheme satisfies the observed rate law, they cannot represent the mechanism of the initial reaction in the absence of air and must be discarded. It becomes necessary to consider other possible mechanisms.

We wish to suggest (Scheme III) that the initial phase of the thermal reduction of MV^{2+} in aqueous solution occurs via the successive attack of OH^- on the 2- and 2′-positions of the two chemically equivalent rings, followed by the reduction of MV^{2+} by the electron-rich double pseudobase (II); the explicit inclusion of ion-paired species, such as [$MV^{2+}\cdots OH^-$], has not been made for the sake of simplicity. It is to be noted that the correct concentration dependence is not obtained if reaction 2 or both reactions 1 and 2 are written as going to completion. By the application of the steady-state approximation to species I and II, the mechanism yields the rate law, $R_i = K_1K_2k_3[MV^{2+}]^2[OH^-]^2$, which is the same as the experimental result when $k_{obsd} = K_1K_2k_3$.

Scheme III

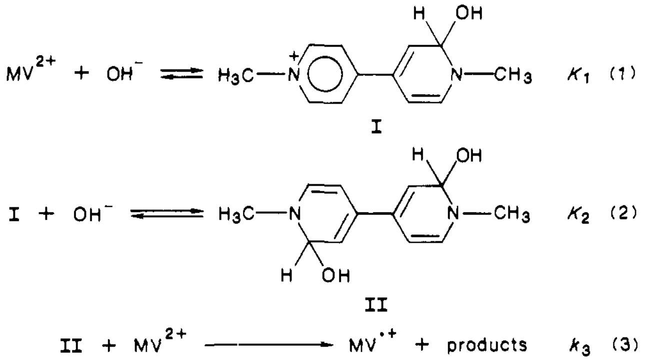

Scheme IV

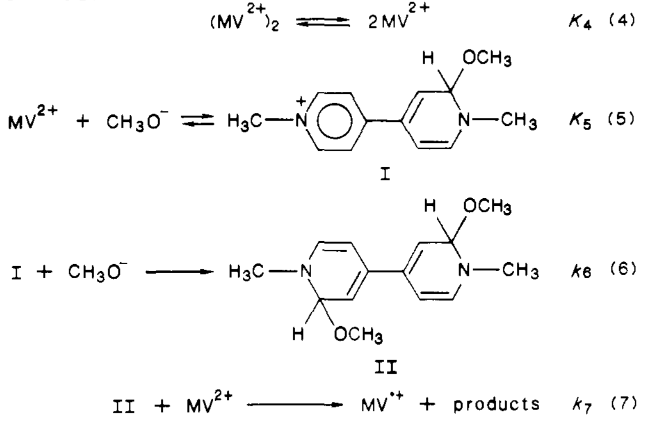

The slowness of the reaction can be attributed to the low values of K_1 and K_2; depending on the redox potential of the double pseudobase and its self-exchange rate, k_3 could exhibit a wide range of values. The result of the low values of K_1 and K_2 is to render the steady-state concentration of the intermediate species very low, perhaps beyond the limits of detectability. The subsequent reactions of the product of the oxidation of intermediate II, here left unspecified, could ultimately lead to many final products. The temperature dependence of k_{obsd} would reflect the dependences of K_1, K_2, and k_3; the apparent activation energy would be equal to ($\Delta H_1° + \Delta H_2° + E_{a3}$). Unfortunately, independent values for these quantities are not available.

When consideration is given to the mechanism of the reaction in methanolic solutions, the first thought is to substitute CH_3O^- for OH^- in Scheme III; inasmuch as CH_3O^- is a stronger base than OH^-, the values of K_1 and K_2 would be expected to be larger, causing the reaction to proceed more rapidly. However, the rate law would remain second-order in both reagents, contrary to the experimental results. The one-half-order in MV^{2+} is especially interesting; such a dependence usually arises from dissociation equilibria. We wish to suggest that MV^{2+} exists in methanolic solutions at the concentrations employed here mainly as a dimeric aggregate, $(MV^{2+})_2$. It is known from light-scattering measurement that MV^{2+} undergoes aggregation in methanol in the millimolar concentration region;[23] inasmuch as the critical aggregation concentration (CAC) in aqueous solution is lowered in highly ionic media, one might expect aggregation to occur in the submillimolar region in methanol. If this is so, the concentration of $(MV^{2+})_2$, then, is essentially one-half that of the MV^{2+} initially introduced into the solution. Thus, the experimental rate law in methanol can be rewritten as $R_i = k_{obsd}'[(MV^{2+})_2]^{1/2}[CH_3O^-]^2$, where $k_{obsd}' = 2k_{obsd}$.

We offer our proposed mechanism for methanolic solutions in Scheme IV. In the first reaction, an equilibrium is established between $(MV^{2+})_2$ and MV^{2+} with $K_1 \ll 1$. However, $(MV^{2+})_2$ is not the reactive species, perhaps for reasons of steric hindrance; rather, CH_3O^- reacts with the MV^{2+} monomer and establishes

---

[23] Ebbesen, T. W.; Ohgushi, M. *Photochem. Photobiol.* 1983, *38*, 251.

an equilibrium with the pseudobase. In contrast with the situation in aqueous solution, the rate law requires that the formation of the double pseudobase proceeds stoichiometrically to completion. It should be noted here that the reduction potential of MV^{2+} is more positive by ~0.1 V in methanol than in water.[24] Thus, Scheme IV results in the rate law $R_i = K_4{}^{1/2}K_5k_6[(MV^{2+})_2]^{1/2}[CH_3O^-]^2$, which is the same as the experimental result when $k_{obsd}' = K_4{}^{1/2}K_5k_6$. The higher rate of the reaction in methanol can be attributed to the greater basicity of CH_3O^- which would result in high values of K_5 and k_6. The apparent activation energy of the reaction in methanol, according to this mechanism, is equal to $((\Delta H_4{}^{\circ})^{1/2} + \Delta H_5{}^{\circ} + E_{a6})$.

Because of the change in mechanism that occurs as the system in mixed solvent solutions transits from water-rich to methanol-rich, R_i is not simply an additive function of the fractional contributions of the rates in the pure solvents. The addition of methanol to water would lower the CAC, thus promoting the aggregation of MV^{2+}, and would provide CH_3O^- to react in competition with OH^- for the formation of the pseudobase intermediates. However, the data in Table III show that R_i is not appreciably affected by the presence of methanol to $X_m \sim 0.1$ (~5 M). Inasmuch as we did not determine the rate law of the reaction as a function of X_m, we cannot speculate further on the mechanism in the mixed solvent region.

In the presence of O_2, reaction 8 occurs rapidly, virtually eliminating any $MV^{\bullet+}$ from solution; $k_8 = 6\text{–}8 \times 10^8$ M^{-1} s^{-1}.[25-27] Reaction 9 represents the oxidation of $MV^{\bullet+}$ by $O_2{}^{\bullet-}$; despite its

$$MV^{\bullet+} + O_2 \rightarrow MV^{2+} + O_2{}^{\bullet-} \qquad (8)$$

$$MV^{\bullet+} + O_2{}^{\bullet-} \rightarrow MV^{2+} + O_2{}^{2-} \qquad (9)$$

$$O_2{}^{\bullet-} + O_2{}^{\bullet-} + 2H_2O \rightarrow O_2 + H_2O_2 + 2OH^- \qquad (10)$$

large rate constant ($k_9 = 9 \times 10^8$ M^{-1} s^{-1}),[26] this reaction cannot be kinetically important in O_2-saturated solutions. For the same reason, the coupling of $O_2{}^{\bullet-}$ with $MV^{\bullet+}$, which is known to occur in aprotic solvents,[28] cannot occur here. $O_2{}^{\bullet-}$ is essentially unreactive and will decay via disproportionation reaction 10 which is very slow in alkaline solution ($k_{10} = 0.3$ M^{-1} s^{-1} at pH 13).[29] Because of the absence of $MV^{\bullet+}$ in oxygenated solutions due to reaction 8, subsequent reactions between $MV^{\bullet+}$ and H_2O_2 can be ignored.[30,31]

Thus, the results in the presence of O_2, whether continuously bubbled, added to a previously deaerated solution, or present as an adventitious impurity in Ar-purged solutions, can be interpreted in terms of the slow formation of H_2O_2 and its subsequent interaction with MV^{2+} which, in aerated alkaline solution, yields a mixture of pyridones.[7] Figures 3 and 4 show that the extent of formation of absorbing and luminescent products is greater when O_2 is bubbled continuously during the reaction period than when O_2 is added to a previously deaerated solution after the same length of time. Clearly, during continuous oxygenation, the formation of H_2O_2 and its subsequent reactions have more time to occur than when the $MV^{\bullet+}$ is quickly scavenged by O_2 and the spectrometric measurements are taken immediately thereafter. The differences in the spectra, aside from the intensities of the bands, when coupled with the melding of a tail absorption into the 380-nm absorption band during continuous oxygenation, testifies to the complexity of the secondary reactions involving H_2O_2. In fact, inasmuch as the characterization of the products in earlier studies[7,8,32] involved large extents of reaction and the presence of O_2, either during the reaction or the analytical workup, it is likely that many of the species observed are the result of secondary processes and do not reflect the initial phases of the reaction.

The exposure of $MV^{\bullet+}$ to air generates luminescent products. Thus, any thermal or photochemical reduction of MV^{2+}, deliberate or inadvertent, in the presence of air will lead to the observation of luminescence. We have pointed out before[18,19] that emission from solutions of MV^{2+}, in the presence or absence of other nonluminescent solutes, arises because the sample of solid MV^{2+} used contains luminescent impurities and/or the air-saturated solutions of MV^{2+} are not handled with the rigorous exclusion of light, especially from UV-emitting fluorescent fixtures in the laboratory. It should be especially noted that MV^{2+} is often recrystallized from alcohols; the presence of minute quantities of alkaline or reducing materials, even from the glassware, would lead rapidly to the formation of the luminescent impurities. These aspects of the system, when coupled with the fact that all reported emissions from MV^{2+} solutions occur with the same λ_{max} regardless of the nature of the other solute, lead us to reiterate our previous conclusion that there is no evidence for bona fide luminescence from MV^{2+} or its complexes.

Acknowledgment. This research was supported by the Office of Basic Energy Sciences, Division of Chemical Sciences, US Department of Energy. We thank Dr. D. R. Prasad for technical assistance.

---

(24) Ledwith, A. In *Biochemical Mechanisms of Paraquat Toxicity*; Autor, A. P., Ed.; Academic: New York, 1977; p 21.

(25) Farrington, J. A.; Ebert, M.; Land, E. J.; Fletcher, K. *Biochim. Biophys. Acta* **1973**, *314*, 372.

(26) Farrington, J. A.; Ebert, M.; Land, E. J. *J. Chem. Soc., Faraday Trans. 1* **1978**, *74*, 665.

(27) Rodgers, M. A. J. *Radiat. Phys. Chem.* **1984**, *23*, 245.

(28) Nanni, E. J., Jr.; Angelis, C. T.; Dickson, J.; Sawyer, D. T. *J. Am. Chem. Soc.* **1981**, *103*, 4268.

(29) Bielski, B. H. J.; Cabelli, D. E.; Arudi, R. L.; Ross, A. B. *J. Phys. Chem. Ref. Data* **1985**, *14*, 1041.

(30) The stoichiometry of the overall reaction between $MV^{\bullet+}$ and O_2 has been recently expressed as $O_2 + 4MV^{\bullet+} + 2H_2O \rightarrow 4MV^{2+} + 4OH^-$.[12] This equation is derived from a scheme in ref 2 (p 330) that includes reactions of $MV^{\bullet+}$ with $O_2{}^{\bullet-}$, H_2O_2, and $^{\bullet}OH$, none of which can be important in solutions containing sufficient O_2.

(31) Levey, G.; Rieger, A. L.; Edwards, J. O. *J. Org. Chem.* **1981**, *46*, 1255.

(32) Corwin, A.; Arellano, R.; Chivvis, A. *Biochim. Biophys. Acta* **1968**, *162*, 533.